journal

J. Am. Ceram. Soc., **82** [11] 3105–12 (1999)

Thermal Conductivity of β-Si_3N_4: I, Effects of Various Microstructural Factors

Mikito Kitayama,*,† Kiyoshi Hirao,*,‡ Motohiro Toriyama,‡ and Shuzo Kanzaki*,‡

Synergy Ceramics Laboratory, Fine Ceramics Research Association, and National Industrial Research Institute of Nagoya, Nagoya, Aichi 463-8687, Japan

Calculations based on a simple modified Wiener's model for thermal conductivity of a composite material predict that the thermal conductivity of β-Si_3N_4 decreases quickly as the grain-boundary film thickness increases within a range of a few tenths of a nanometer and also that it initially increases steeply with increased grain size, then reaches almost constant values. Because of the faceted nature of the β-Si_3N_4 crystal, the "average" grain-boundary film thickness is much greater than that in equilibrium. The present study demonstrates both theoretically and experimentally that grain growth alone cannot improve the thermal conductivity of β-Si_3N_4.

I. Introduction

ALTHOUGH intensive studies have improved the thermal conductivity of AlN to near the intrinsic value (319 W/(m·K)) in the past decade, the poor mechanical properties of the compound, in addition to the high production cost, have kept it from wide commercial use. SiC, another candidate for high thermal conductivity, is not appropriate for electrical use because of its electrical conductivity. Electrical industries have strongly desired an alternative material with high thermal conductivity for electrical-substrate applications, in order to deal with heat from an ever-increasing number of electrical devices. Haggerty and Lightfoot[1] pointed out Si_3N_4 as a material with potentially high thermal conductivity (200–320 W/(m·K)) at room temperature. The superior mechanical and electrical properties of Si_3N_4 make it an excellent prospective material for electrical substrates. Improving the thermal conductivity of Si_3N_4 also is crucial for its application in automotive engines, where good thermal-shock resistance is required. However, relatively poor thermal-conductivity values, ranging from 20 to 70 W/(m·K), have been reported for Si_3N_4 ceramics fabricated by reaction bonding,[2,3] chemical vapor deposition (CVD),[4] hot-pressing,[2,5,6] and hot-isostatic-pressing methods.[7,8] Hayashi *et al.*[9] developed an α-Si_3N_4 with a high thermal conductivity of 110–150 W/(m·K) through the CVD process, by carefully controlling the oxygen content. Unfortunately, this material exhibited very poor mechanical properties, probably because of its extremely large grains (in the millimeter range) and lack of a grain-boundary phase.

Very recently, the thermal conductivity of liquid-phase-sintered β-Si_3N_4 has exceeded 100 W/(m·K). Hirao *et al.*[10] fabricated an Si_3N_4 with a highly anisotropic microstructure and exhibiting high thermal conductivity—up to 120 and 60 W/(m·K)—by rendering rodlike β-Si_3N_4 seed particles, arranged unidirectionally via tape casting, into orientations parallel and perpendicular, respectively, to the tape-casting direction after annealing at 1850°C for up to 66 h under a nitrogen pressure of 1 MPa. Watari *et al.*[11] further annealed this material at 2500°C under a nitrogen pressure of 200 MPa, and the thermal conductivity reached 155 and 52 W/(m·K) in the orientations parallel and perpendicular, respectively, to the tape-casting direction. Hirosaki *et al.*[12,13] achieved high thermal conductivity, up to 120 W/(m·K), by annealing β-Si_3N_4 at 2000°–2200°C for 4 h under high nitrogen pressures (10–100 MPa) to prevent the decomposition of Si_3N_4 (gas-pressure-sintering).

In those works, grain growth of β-Si_3N_4 promoted by prolonged annealing time or extremely high annealing temperature was the key factor for improving thermal conductivity. Based on experimental results, Hirosaki *et al.*[12,13] stressed that the amount of grain-boundary film directly related to grain size might significantly influence the thermal conductivity of β-Si_3N_4. Assuming unidirectionally arranged, elongated β-grains as continuous fibers, Hirao *et al.*[10] demonstrated that the relationship between the area fraction of elongated grains and thermal conductivity accurately follows Wiener's parallel and serial formulas for the thermal conductivity of a composite material.[14]

Although Wiener's formulas might be applicable to β-Si_3N_4 with a bimodal structure consisting of a fine matrix and large elongated grains, they are not sufficient to describe the thermal conductivity of β-Si_3N_4 without such a unique microstructure. The formulas contain only the volume fractions of constituents and cannot treat the grain sizes (width and length), arrangement of anisotropic grains, and grain-boundary glassy film that all characterize β-Si_3N_4.

Buhr and Müller[15] treated the thermal conductivity of AlN using simple cubic models with thin grain-boundary films and with or without a continuous network of secondary phases along the grain edges. Those calculated thermal conductivities were in good agreement with the above-mentioned measured values of AlN sintered bodies with two types of microstructures.[15,16] Because the grain shape of AlN was isotropic, simple cubic models could successfully simulate the thermal conductivity of this material. Although the grain-boundary film thickness was taken into account in that model, grain anisotropy was not considered, so that the model is not applicable to β-Si_3N_4 with a highly anisotropic grain shape.

The strong tendency toward faceting of liquid-phase-sintered Si_3N_4 further complicates the modeling of the thermal conductivity of β-Si_3N_4. Even though the distance between two crystals is in equilibrium (typically 1–2 nm)[17] for some of the crystals, other parts should have much greater distances because the prismatic planes of β-Si_3N_4 facet when the two elongated grains are not parallel but inclined to each other, as in a general case.

The purpose of the present work is to model the thermal

T. A. Parthasarathy—contributing editor

Manuscript No. 189611. Received January 20, 1999; approved May 19, 1999.

This work was conducted as part of the Synergy Ceramics Project, under the Industrial Science and Technology Frontier (ISTF) program promoted by the Agency of Industrial Science and Technology (AIST), Ministry of International Trade and Industry (MITI), Japan. Part of the work under this program was funded through the New Energy and Industrial Technology Development Organization (NEDO). The authors are members of the Joint Research Consortium of Synergy Ceramics.

*Member, American Ceramic Society.

†Author to whom correspondence should be addressed.

‡National Industrial Research Institute of Nagoya.

conductivity of β-Si_3N_4, taking into account grain sizes (width and length), the arrangement of anisotropic grains, and the grain-boundary film thickness, and to provide experimental data supporting the proposed model. The effects of various microstructural factors are discussed in conjunction with the unique faceting nature of β-Si_3N_4.

II. Modeling

Anisotropy in thermal conductivity is described well by Wiener's[14] parallel and serial formulas for the thermal conductivity of a composite material, as follows,

$$\text{Parallel arrangement} \qquad k_p = V_1k_1 + V_2k_2 \tag{1}$$

$$\text{Serial arrangement} \qquad \frac{1}{k_s} = \frac{V_1}{k_1} + \frac{V_2}{k_2} \tag{2}$$

where k_1 and k_2 are the thermal conductivities of components 1 and 2, respectively, and V_1 and V_2 the volume fractions of components 1 and 2, respectively.

Figure 1 shows an idealized two-dimensional microstructure of β-Si_3N_4, in which the (001) and (100) planes of the β-crystals are perfectly oriented to the directions designated *para* and *perp*, respectively. Each grain has an equal width (distance between the two opposite (100) facets) and length (distance between the two opposite (001) facets), w and l, respectively. Assume that the grain-boundary film thickness, δ, is independent of the crystallographic orientations and completely covers the grain surfaces. If the amount of grain-boundary glassy phase exceeds that required for complete covering of the grains, the rest exists as glass pockets, as shown in Fig. 1. When the volume fraction of the glassy phase equals x, the volume fraction of the glass pockets, f_p, is

$$f_p = x - \frac{\delta(w+l)}{wl}(1-x) \tag{3}$$

Using the well-known Maxwell's relationship for the thermal conductivity of composite materials with a dispersed secondary phase,[18] the thermal conductivity of the Si_3N_4 matrix, k_m, with dispersed glass pockets is expressed as

$$k_m = k_c \frac{1 + 2f_p \dfrac{1-Q}{2Q+1}}{1 - f_p \dfrac{1-Q}{2Q+1}} \tag{4}$$

where k_c and Q are the thermal conductivity of the crystal and the thermal-conductivity ratio of the β-Si_3N_4 crystal and the grain-boundary glassy phase, k_c/k_g, respectively. Although thermal-conductivity anisotropy might exist, depending on the crystallography of the β-Si_3N_4, we assume in this work that the thermal conductivity is independent of the crystallography. To take grain sizes (width and length) and grain-boundary film thickness into account, we modify the Wiener's parallel and serial formulas for the thermal conductivity of a composite material. For the para orientation, the thermal conductivity, k_{para}, can be expressed by combining the following two equations.

$$k'_m = \frac{l}{l+\delta}k_m + \frac{\delta}{l+\delta}k_g \tag{5a}$$

$$\frac{1}{k_{para}} = \frac{w}{w+\delta}\frac{1}{k'_m} + \frac{\delta}{w+\delta}\frac{1}{k_g} \tag{5b}$$

For the perp orientation, the thermal conductivity, k_{perp}, can be expressed likewise,

$$k''_m = \frac{w}{w+\delta}k_m + \frac{\delta}{w+\delta}k_g \tag{6a}$$

$$\frac{1}{k_{perp}} = \frac{l}{l+\delta}\frac{1}{k''_m} + \frac{\delta}{l+\delta}\frac{1}{k_g} \tag{6b}$$

where k'_m and k''_m are the composite thermal conductivities when grains and grain-boundary films are arranged serially along the para and perp orientations, respectively. Combining

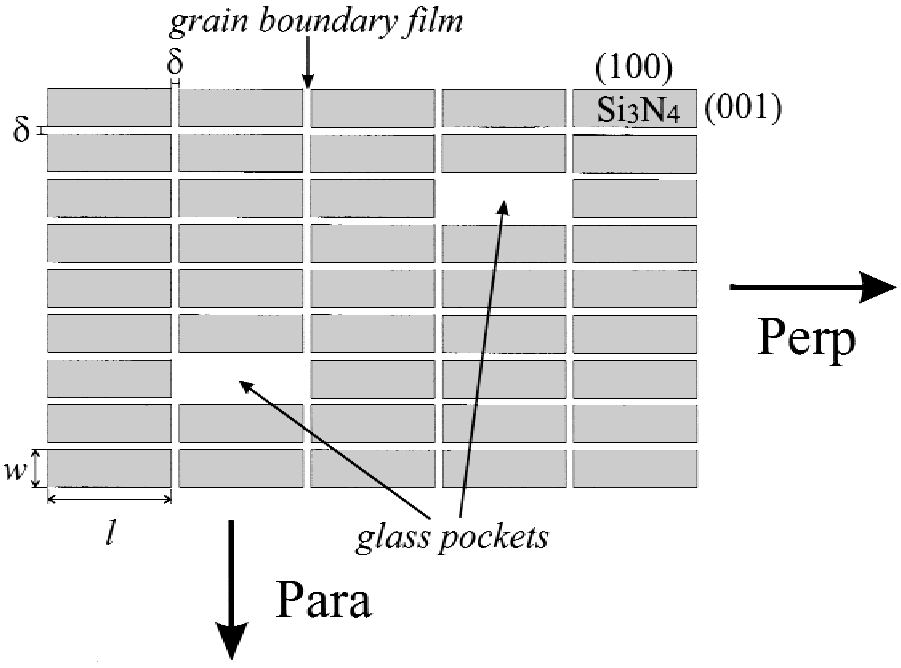

Fig. 1. Illustration of idealized two-dimensional microstructure of β-Si_3N_4; [210] and [001] directions of β-grains are perfectly oriented to directions designated para and perp, respectively; grain-boundary film thickness, δ, is independent of crystallographic orientations and completely covers grain surfaces. If the amount of grain-boundary glassy phase exceeds that required for complete covering of grains, remainder is assumed to exist as glass pockets.

Eqs. (3)–(6) makes it possible to describe the thermal conductivity of β-Si_3N_4, taking into account grain sizes (width and length), the arrangement of anisotropic grains, and the grain-boundary film thickness.

III. Experimental Procedure

Commercially available submicrometer-sized β-Si_3N_4 powder (SN-21FC grade, β-phase content 100%, average particle size 0.55 μm, oxygen content 0.47 wt%; Denki Kagaku Kogyo Co., Tokyo, Japan) was ultrasonically dispersed into distilled water containing 1 wt% dispersing agent (A-6114, Toagosei Co., Ltd., Tokyo, Japan). The resultant slurry was classified by centrifugal sedimentation at 1500*g* for 5 min, which made particles >0.5 μm settle out completely. The supernatant was separated from the sediment and consolidated, using a centrifuge at 3000*g* for 10 min. The sediment was dispersed in ethanol and consolidated again, using a centrifuge at 2000*g* for 5 min. This procedure then was repeated, using acetone, after which the samples were dried at 110°C for 2 h and passed through a 60-mesh nylon sieve. The resultant powder was designated submicrometer β-powder.

The submicrometer β-powder and two commercial α-Si_3N_4 powders (SN-E10, specific surface area 9–13 m^2/g, and SN-E05, specific surface area 4–6 m^2/g, oxygen content <2.0 wt%; UBE Industries, Ltd., Yamaguchi, Japan) were each mixed with 5 wt% Y_2O_3 powder (purity >99.9%, specific surface area 27 m^2/g; Hokko Chemical Industry Co., Ltd., Tokyo, Japan) in a resin-coated ball mill for 3 h, using methanol as a mixing medium. Each slurry was dried, using a rotary evaporator, at 60°C, then dried at 110°C for 2 h and passed through a 60-mesh nylon sieve. A measured quantity of each mixed powder (30 g) was charged into a 30 mm high-purity graphite dye (Toyotanso Co., Osaka, Japan) coated with high-purity BN powder (GP grade, Denki Kagaku Kogyo Co.).

The submicrometer β-powder and the α-Si_3N_4 powders were hot-pressed at 1800°C for 30 min and 2 h, respectively, under a pressure of 40 MPa in a flowing nitrogen atmosphere. Those conditions produced sintered bodies with >99% of theoretical density. The hot-pressed β-Si_3N_4 made from the α-Si_3N_4 powders then was annealed at 1850°C for 4 and 16 h, under a nitrogen pressure of 1 MPa, in a high-purity BN crucible (N1 grade, Denki Kagaku Kogyo Co.) with a mixed powder bed of Si_3N_4 (UBE SN-E10) and BN (GP grade, Denka, Tokyo, Japan) in the ratio 7:3. Both hot-pressing and annealing were conducted in a furnace with graphite heating elements that had never been used for materials containing aluminum. Extreme care was taken to avoid any possible contamination by combining the described treatment with the use of a resin-coated ball mill and a high-purity graphite dye.

Phase identification of the sintered body was performed by X-ray diffractometry (XRD). Disk samples 10 mm in diameter and 2 mm thick, for measuring thermal properties (thermal diffusivity and specific heat) were taken from all of the sintered samples, parallel and perpendicular to the hot-pressed surfaces, and designated the para and perp samples, respectively, as illustrated in Fig. 2; these samples were finished using a No. 200 wheel.

Sample densities were determined by the Archimedes method. The thermal properties were measured by the laser-flash method (Model TC-3000, ULVAC Japan, Ltd., Kanagawa, Japan) after both sides of the samples had been coated with a 600 Å thickness of gold and then with black carbon layers. The thermal conductivity, k, was calculated according to the equation, $k = \rho C_p \alpha$, where ρ, C_p, and α are the density, specific heat, and thermal diffusivity, respectively. After the thermal properties had been measured, all of the disk samples were finished, using 1 μm diamond slurry, then plasma-etched in CF_4 gas, coated with a 200 Å thickness of gold, and observed by scanning electron microscopy (SEM; Model JSM-6340F, JEOL, Tokyo, Japan). The mean grain sizes were determined from SEM photographs, using the linear-intercept method.

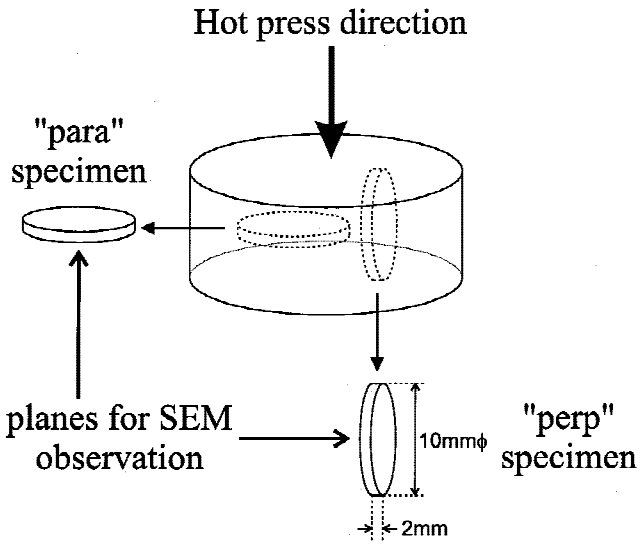

Fig. 2. Illustration showing how disk specimens (10 mm × 2 mm) were taken from sintered samples; disk surfaces of para and perp specimens were oriented perpendicular and parallel, respectively, to hot-pressing direction. Shown are planes for SEM observation and planes irradiated by laser beam when thermal properties were measured (heat flows in the directions perpendicular to specimen surfaces).

IV. Results

Figures 3–5 show SEM photographs of β-Si_3N_4 fabricated from the submicrometer β-powder (hot-pressed at 1800°C for 30 min) and the SN-E10 and SN-E05 powders (hot-pressed at 1800°C for 2 h, then annealed at 1850°C for 4 h), respectively. In all figures, (a) and (b) designate the para and perp samples, respectively.

Figure 3 demonstrates that the submicrometer size of the raw powder was maintained successfully because of the lack of α–β transformation and a shorter hot-pressing time. Figure 5 shows the extremely large grain size of the β-Si_3N_4. This size probably is attributable to use of the SN-E05 powder, which contains much fewer β-nuclei than does the SN-E10.

Figure 4 shows the typical microstructure of β-Si_3N_4, familiar from previous works because UBE SN-E10 commonly is used as the starting powder for fabricating Si_3N_4 sintered bodies. The β-Si_3N_4 grain size is halfway between those shown in Figs. 3 and 5. Hence, β-Si_3N_4 sintered bodies with an extremely wide range of grain size were successfully obtained. The difference between photographs (a) and (b) is significant in all figures: The elongated β-grains in the (a) photographs lie nearly along the hot-pressed surfaces, showing mainly prismatic facets. In contrast, fewer elongated grain shapes are observed in (b), and hexagonal grain shapes are the main feature in these photographs. As a result, the (a) microstructures are much more anisotropic than the (b). This difference in microstructure results from the alignment of the rodlike β-Si_3N_4 grains during uniaxial pressing.

Table I shows the mean grain sizes and thermal conductivities of all the para and perp samples. As shown in Fig. 2, the measured thermal conductivities are the values perpendicular to the planes observed by SEM; hence, the mean grain sizes of the para and perp samples correspond to the thermal conductivities of the perp and para samples, respectively. The differences in grain size between the para and the perp samples are quite small, probably because of the method used for determining grain sizes. The figures determined by the linear-intercept method are very close to the grain width, because of the rodlike grain shape of the β-Si_3N_4.

Table I reveals that the thermal conductivity of β-Si_3N_4 increases as grain size increases. The thermal conductivity also demonstrates a significant dependence on sample orientation.

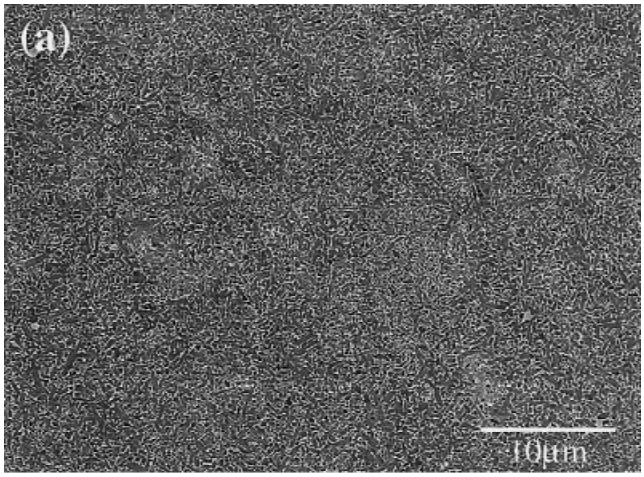

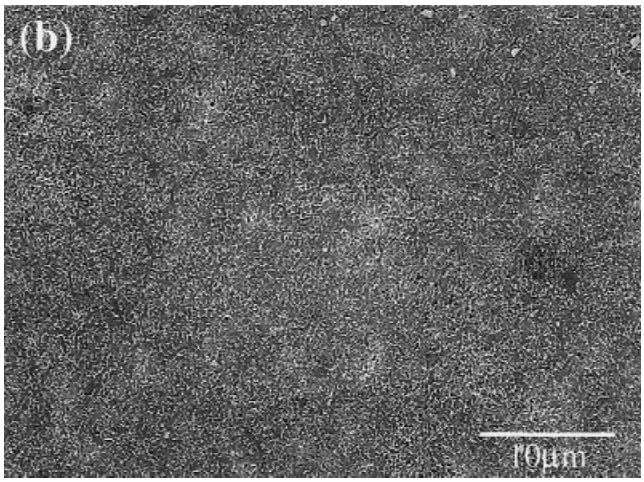

Fig. 3. SEM photographs of β-Si_3N_4 fabricated from submicrometer β-powder hot-pressed at 1800°C for 30 min: (a) planes parallel and (b) planes perpendicular to hot-pressing surface.

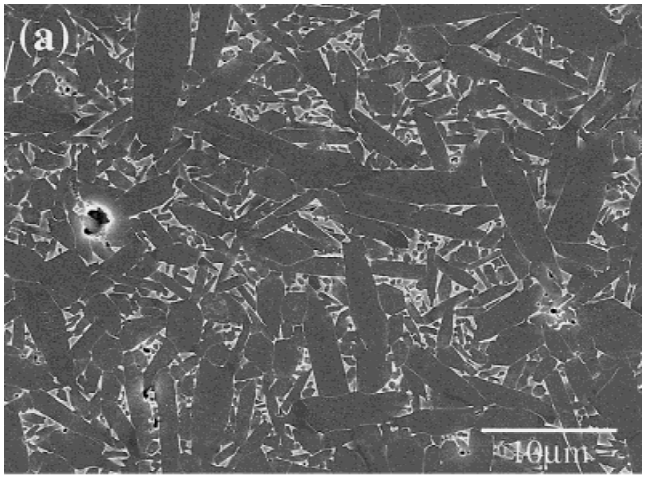

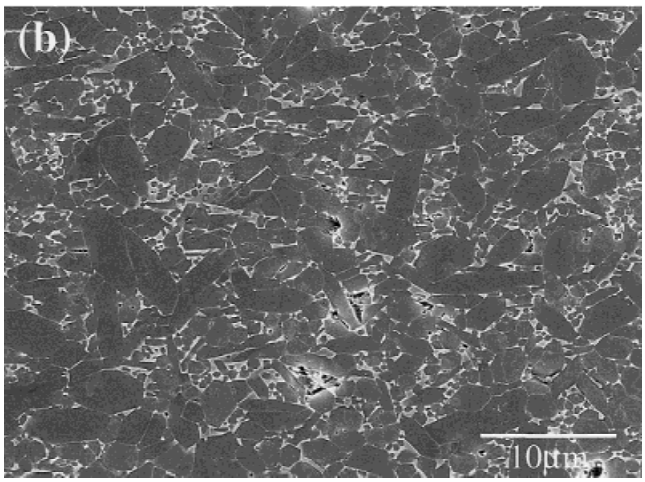

Fig. 4. SEM photographs of β-Si_3N_4 fabricated from SN-E10 hot-pressed at 1800°C for 2 h, then annealed at 1850°C for 4 h: (a) planes parallel and (b) planes perpendicular to hot-pressing surface.

The thermal conductivities of the para samples always are smaller than those of the perp samples. Because the elongated β-grains lie along the hot-pressed surfaces, as shown in Figs. 3–5, the thermal conductivities of the para and perp samples correspond to those of the para and perp orientations shown in Fig. 1.

Figure 6 shows the relationship between mean grain size and thermal conductivity for the β-Si_3N_4 samples. When the mean grain size is plotted using a logarithm scale, a good straight line can be drawn for the plots of the experimental data, suggesting an apparent exponential dependence of thermal conductivity on mean grain size, as follows,

$$k = C_1 \ln (d) + C_2 \tag{7}$$

where C_1 and C_2 are constants and d the mean grain size. However, this relationship is just phenomenological and has no theoretical meaning, because the thermal conductivity becomes negative and infinite when the line is extrapolated to both sizes, which should never happen. This result suggests that the apparent linear relationship involves some effects other than mere grain size.

V. Discussion

Table II summarizes the difference between AlN and β-Si_3N_4 from the aspect of thermal conductivity. Although the compounds are quite similar in many points, including the intrinsic thermal conductivity, the nature of faceting in β-Si_3N_4 significantly differentiates it, as mentioned already in the Introduction. Even though the distance between two crystals is in equilibrium in parts of the crystals, other parts should have much greater distances, because the prismatic planes of the β-Si_3N_4 facet when the two elongated grains are not parallel but rather inclined to each other, as in a general case.

Figure 7, an enlarged SEM photograph of Fig. 4(a), accurately illustrates this concept. The part of the grain boundary indicated by (△) is quite thin and would have the equilibrium grain-boundary thickness. In contrast, the other part, indicated by (▲), is much wider, because of faceting of the prismatic planes of the β-Si_3N_4, and is called here the thick film, in contrast to the thin film in equilibrium. The thick films clearly behave differently from the dispersed glassy pockets, a factor that should significantly affect the thermal conductivity resulting from the filmlike morphology.

The model proposed in the present work predicts how grain-boundary thickness affects the thermal conductivity of β-Si_3N_4. Calculations were performed using the thermal conductivity values of 180 and 1 W/(m·K) for the β-Si_3N_4 crystal and the grain-boundary glassy phase, respectively. Hirao *et al.*[10] predicted an intrinsic thermal-conductivity value of 180 W/(m·K) by extrapolating the relationship between the area fraction of elongated grains and the thermal conductivity. This value was chosen here for the thermal conductivity of the β-Si_3N_4 crystal because the same additive (5 wt% Y_2O_3) was used in the present study.

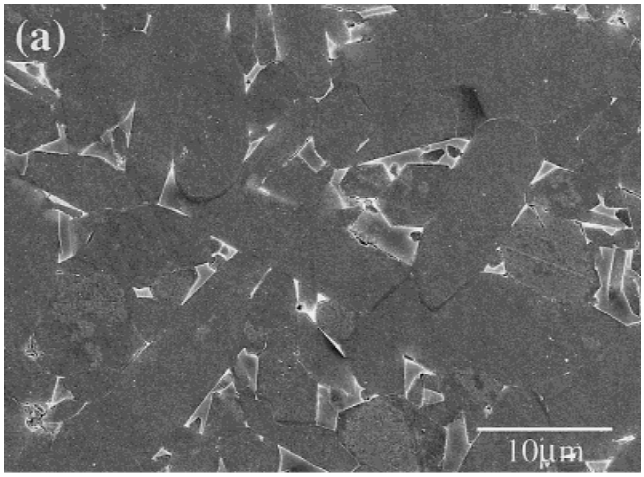

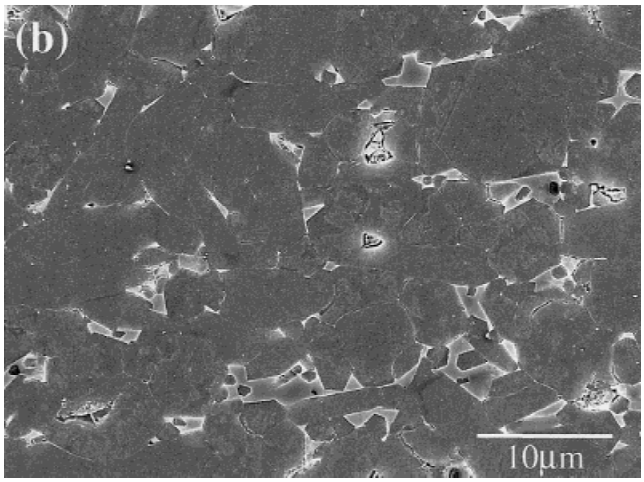

Fig. 5. SEM photographs of β-Si_3N_4 fabricated from SN-E05 hot-pressed at 1800°C for 2 h, then annealed at 1850°C for 4 h: (a) planes parallel and (b) planes perpendicular to hot-pressing surface.

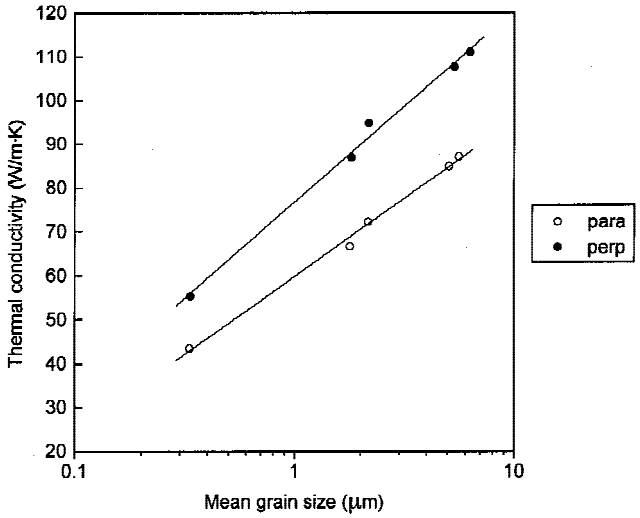

Fig. 6. Relationship between mean grain sizes and thermal conductivities of β-Si_3N_4 sintered bodies. Note: A straight line can be drawn for plots of experimental data when mean grain sizes are plotted using a logarithm scale.

A typical thermal-conductivity value for silicate-based glass is as low as 1 W/(m·K).[19] Figure 8 shows the effect of grain-boundary thickness on the thermal conductivity of β-Si_3N_4 when the grain width and length are 1 and 5 μm, respectively; the grain aspect ratio, $R = l/d$, is 5; and the volume fraction of glassy phase, x, is 6%. In the case of the grain-boundary film thickness, $\delta = 0$ nm, all of the glassy phase exists as dispersions, and the thermal conductivity decreases from the intrinsic value, 180 W/(m·K), to 164.4 W/(m·K). The thermal conductivity decreases slightly, to 141.5 and 159.3 W/(m·K), for the para and perp orientations, respectively, when $\delta = 1$ nm, a typical value in equilibrium. The thermal conductivity decreases noticeably, to 63.2 and 124.6 W/(m·K), for the para and perp orientations, respectively, when $\delta = 10$ nm. High anisotropy in thermal conductivity is observed in this second case.

Figure 8 demonstrates that the thermal conductivity of β-Si_3N_4 is affected significantly by the grain-boundary film thickness, within a range of a few tenths of a nanometer. Figure 8 also shows that thermal-conductivity anisotropy can arise through the arrangement of anisotropic β-grains, which directly changes the number of thin films per unit thickness. In AlN, the homogeneous thickness of the grain-boundary amorphous film, if it exists, is in the range 2–4 nm[15] because of the isotropic nature of the AlN crystal. Because of the thin and homogeneous film thickness, the thermal conductivity of AlN is affected by as little as −5%–10%, which explains why the oxygen content dissolved in the AlN lattice has a dominant influence in AlN ceramics. In β-Si_3N_4 ceramics, however, the grain-boundary film should significantly influence the thermal conductivity because of the thick film, as shown in Fig. 7. An averaged thickness of the thin (in equilibrium) and thick films would influence the thermal conductivity of β-Si_3N_4 on the whole. Figure 8 demonstrates that this effect is enormous.

Figure 9 shows the effect of grain size on the thermal conductivity of β-Si_3N_4 when $R = 5$ for the β-grain and $x = 6\%$. The calculations were performed using grain-boundary film thickness values of 1, 10, and 50 nm. Figure 9 demonstrates that the thermal conductivities of β-Si_3N_4 initially increase steeply as grain size increases, up to certain values dependent on film thickness, and then remain almost constant. This trend

Table I. Mean Grain Sizes and Thermal Conductivities of Samples Taken Parallel and Perpendicular to Hot-Pressed Surfaces of Sintered β-Si_3N_4

Sample	Hot-pressing conditions	Annealing conditions	Sample orientation	Mean grain size (μm)	Thermal conductivity (W/(m·K))
Submicrometer β-powder	1800°C, 30 min		para	0.335	43.5
			perp	0.332	55.4
UBE SN-E10	1800°C, 2 h	1850°C, 4 h	para	1.82	66.7
			perp	1.79	87.0
		1850°C, 16 h	para	2.19	72.3
			perp	2.17	94.9
UBE SN-E05	1800°C, 2 h	1850°C, 4 h	para	5.37	85.0
			perp	5.07	107.7
		1850°C, 16 h	para	6.30	87.2
			perp	5.64	111.1

Table II. Comparison of β-Si_3N_4 and AlN Ceramics in Terms of Thermal Conductivity

	β-Si_3N_4	AlN
Chemistry	Si^{4+} Ionic radius: 0.26 Å Electronegativity: 1.90	Al^{3+} Ionic radius: 0.39 Å Electronegativity: 1.61
Crystallography	Hexagonal ($P6_3$)	Hexagonal (wurtzite)
Melting point	1850°C–decomposition	2000°C–sublimation
Intrinsic thermal conductivity	200 or 320 W/(m·K)[†]	319 W/(m·K)
Secondary phase (thermal conductivity)	Mainly amorphous (~1 W/(m·K))	Mainly crystalline (~10 W/(m·K))
Morphology of GBP	Thin film Glass pocket	Thin film Grain edge Dispersion
Oxygen solid solution	NA	0.05–0.5 wt%[‡]
Highest thermal conductivity reported	155 W/(m·K)[‡]	~260 W/(m·K)[§]

[†]Haggerty and Lightfoot (Ref. 1) predicted that 320 W/(m·K) would be a more probable value. [‡]Reference 11. [§]Reference 22.

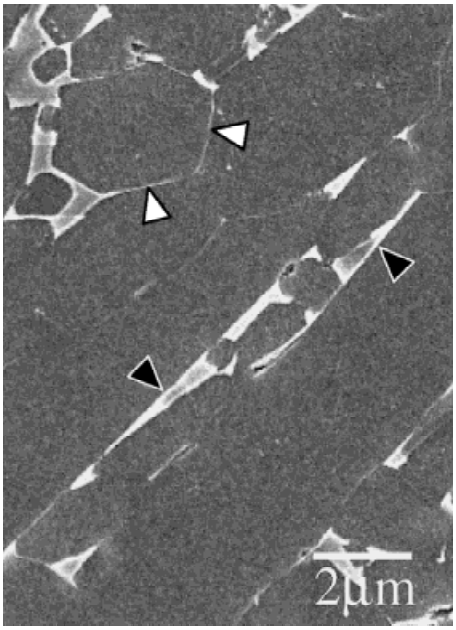

Fig. 7. Enlargement of SEM photograph in Fig. 3(a): Part of grain boundary indicated by (△) is very thin, with equilibrium grain-boundary thickness; (▲) is much wider because of faceting of prismatic planes of β-Si_3N_4.

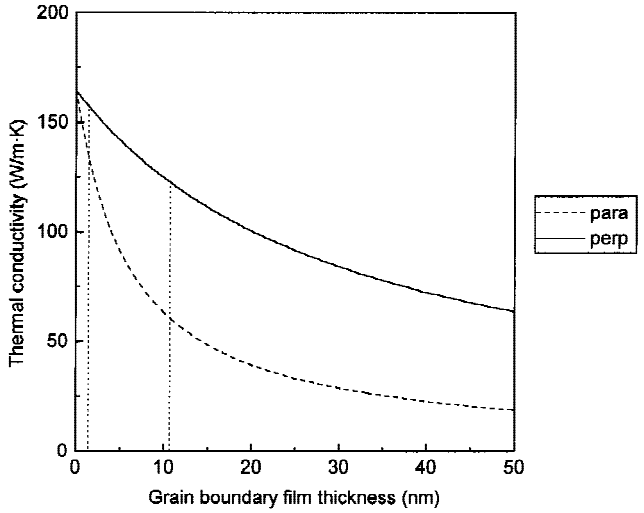

Fig. 8. Effect of grain-boundary thickness on thermal conductivity of β-Si_3N_4 for $d = 1$ μm, $l = 5$ μm ($R = 5$), and $x = 6\%$.

suggests that grain growth promoted by excess heat treatments improves thermal conductivity very little. That fact does not negate the importance of purification promoted by dissolution and reprecipitation during Ostwald ripening; however, grain growth alone does not significantly improve the thermal conductivity of β-Si_3N_4 once grain size reaches certain critical values (for example, ~1 μm when the grain-boundary film thickness is 1 nm).

Figure 9 reveals that a more important way of improving thermal conductivity is to reduce the average grain-boundary film thickness—that is, to reduce the tendency toward faceting. The high toughness of Si_3N_4 ceramics derives from elongated grains[20] developed because of the faceting nature of β-Si_3N_4 crystals,[21] so that improving thermal conductivity may conflict with improving toughness. However, if grain growth is not necessary for improving thermal conductivity, β-Si_3N_4 may be usable as a substrate material because a coarse grain size drastically decreases β-Si_3N_4 strength[9] and also because increased production costs resulting from excess heat treatments can be avoided. The anisotropy of thermal conductivity (the difference between the para and the perp orientations) does increase with increased grain-boundary film thickness.

In contrast to the grain-boundary films, the grain-boundary glassy phase that exists as glass pockets has much less of an effect on thermal conductivity. Figure 10 illustrates the effect of the volume fraction of glassy phase on the thermal conductivity of β-Si_3N_4 with $R = 1$ for the β-grains and grain-boundary film thicknesses of $\delta = 1$ and $\delta = 10$ nm. Calculations were performed for 2%, 4%, 6%, 8%, and 10% volume fractions of glassy phase, typical amounts for β-Si_3N_4. Increasing the volume fractions of glassy phase from 2% to 10% decreased the thermal conductivity by only 20 W/(m·K). Compared to the effect of the grain-boundary film thickness (1 versus 10 nm), the effect of the glass pockets was insignificant. This difference suggests that an effort to reduce glass content while sacrificing sinterability has little effect. Again, these results confirm that film thickness is a dominant factor affecting the thermal conductivity of β-Si_3N_4.

After improving our understanding of the thermal conductivity of β-Si_3N_4 through the above-mentioned calculations, we analyzed the experimental results for the present work. From the amount of Y_2O_3 additive and oxygen content in the raw powders, the volume fraction of glassy phase was assumed to be ~6%. The aspect ratio of the β-grains was taken as $R = 2$ for all samples, close to the measured average values. Using the thermal-conductivity values for β-Si_3N_4 crystal and glass mentioned previously, calculations were performed to find the best fit to the experimental results.

Figure 11 compares the calculated and experimental results and suggests that the grain-boundary film thickness values are ~7, ~19, and ~35 nm for samples fabricated from the submicrometer powders, the UBE SN-E10, and the SN-E05, respectively. These values may vary, depending on the intrinsic thermal-conductivity values assumed for the β-Si_3N_4 crystal. However, the implication that the grain-boundary film thickness increases with increased grain size remains unaltered.

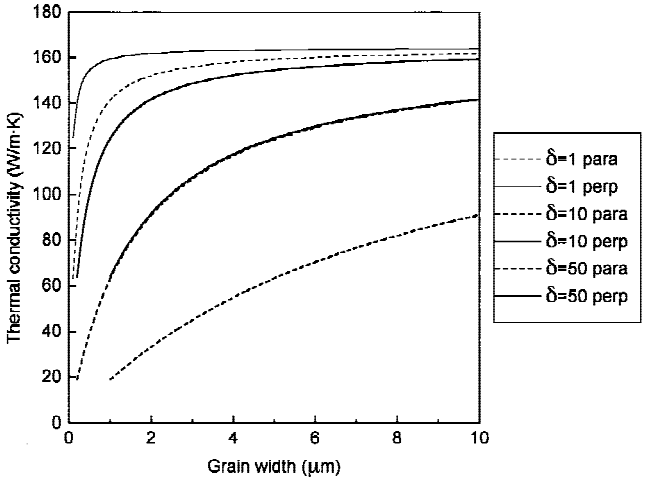

Fig. 9. Effect of grain size on thermal conductivity of β-Si_3N_4 with various grain-boundary film thickness values, for $R = 5$ in β-grain and $x = 6\%$.

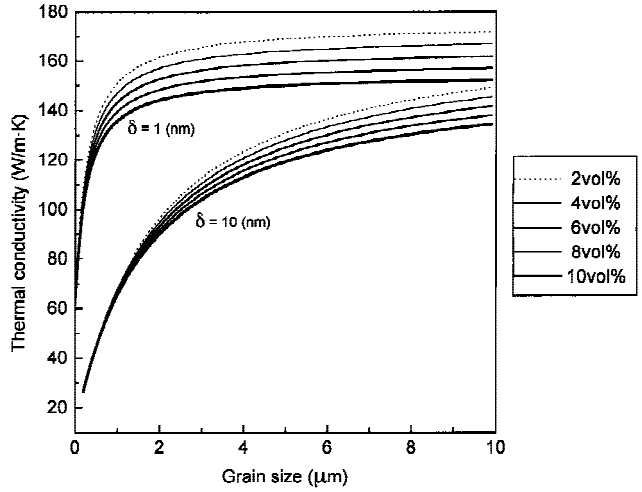

Fig. 10. Effect of volume fraction of glassy phase on thermal conductivity of β-Si_3N_4 for $R = 1$ in β-grain and $\delta = 1$ and 10 nm.

Here, the effect behind the apparent linear relationship between the logarithm of the mean grain size and the thermal conductivities observed in Fig. 6 is clarified.

Thus, the average grain-boundary film thickness understandably increases with grain size. Assuming that the average angle between two adjacent prismatic planes of β-Si_3N_4 is independent of grain size, the average distance between two adjacent β-grains is a function of grain size. We have already mentioned that promoting grain growth to improve the thermal conductivity of β-Si_3N_4 increases the average grain-boundary film thickness. Again, grain growth alone proves incapable of improving the thermal conductivity of β-Si_3N_4. A knowledge of AlN ceramics[22] indicates that the thermal conductivity of β-Si_3N_4 might be improved significantly by reducing the oxygen content dissolved in the lattice. Because no reports have treated the oxygen content of β-Si_3N_4, further fundamental studies on this subject certainly are necessary in the future.

VI. Conclusions

The faceting nature of a β-Si_3N_4 crystal causes the "average" grain-boundary film thickness to be much larger than that in equilibrium. This size difference may be one of the main reasons that the known thermal conductivities of β-Si_3N_4 are much smaller than those of AlN with a thin grain-boundary film of homogeneous thickness. The following conclusions can be drawn from the present work.

(1) The thermal conductivity of β-Si_3N_4 is strongly dependent on the average grain-boundary film thickness, within the range of a few tenths of a nanometer.

(2) The thermal conductivity of β-Si_3N_4 initially increases steeply with increased grain size, then reaches almost constant values above certain critical grain sizes determined by the grain-boundary thickness and the amount of glassy phase.

(3) Thermal conductivity anisotropy can emerge from an arrangement of anisotropic β-grains.

(4) The average grain-boundary film thickness increases as grain size increases.

Overall, the present work has elucidated the relationship between thermal conductivity and various microstructural factors in β-Si_3N_4 and has demonstrated that grain growth alone cannot improve the thermal conductivity of β-Si_3N_4 exceeding certain critical grain sizes.

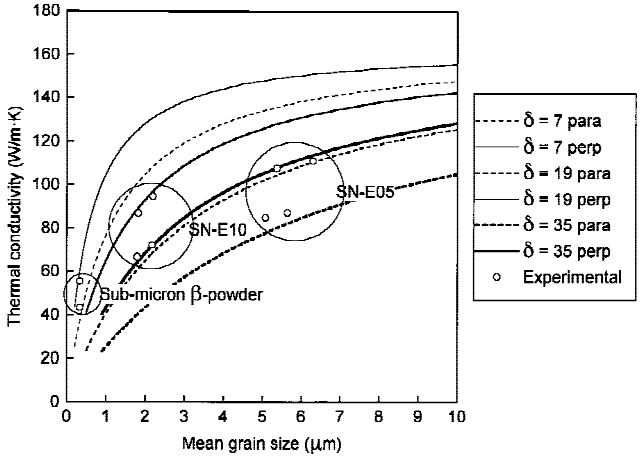

Fig. 11. Effect of grain size on thermal conductivity of β-Si_3N_4 with various grain-boundary film thickness values, comparing experimental data and best-fit calculations for $R = 2$ in β-grain and $x = 6\%$; best-fit values of grain-boundary film thickness are 7, 19, and 35 nm for samples fabricated from submicrometer β-powder, SN-E10, and SN-E05, respectively.

References

[1]J. S. Haggerty and A. Lightfoot, "Opportunities for Enhancing the Thermal Conductivities of SiC and Si_3N_4 Ceramics through Improved Processing," *Ceram. Eng. Sci. Proc.*, **16** [4] 475–87 (1995).

[2]G. Ziegler and D. P. H. Hasselman, "Effect of Phase Composition and Microstructure on the Thermal Diffusivity of Silicon Nitride," *J. Mater. Sci.*, **16**, 495–503 (1981).

[3]K. Hayashi, S. Tsujimoto, T. Nishikawa, and Y. Imamura, "Thermal Conductivity of Reaction-Bonded Si_3N_4," *Yogyo Kyokaishi*, **94** [6] 595–600 (1986).

[4]T. Hirai, S. Hayashi, and K. Niihara, "Thermal Diffusivity, Specific Heat, and Thermal Conductivity of Chemically Vapor-Deposited Si_3N_4," *Am. Ceram. Soc. Bull.*, **57** [12] 1126–30 (1978).

[5]M. Kuriyama, Y. Inomata, T. Kijima, and Y. Hasegawa, "Thermal Conductivity of Hot-Pressed Si_3N_4 by Laser-Flash Method," *Am. Ceram. Soc. Bull.*, **57** [12] 1119–22 (1978).

[6]K. Tsukuma, M. Shimada, and M. Koizumi, "Thermal Conductivity and Microhardness of Si_3N_4 with and without Additives," *Am. Ceram. Soc. Bull.*, **60** [9] 910–12 (1981).

[7]K. Watari, Y. Seki, and K. Ishizaki, "Thermal Properties of HIP-Sintered Silicon Nitride," *J. Ceram. Soc. Jpn.* (*Yogyo Kyokaishi*), **97** [1] 56–62 (1989).

[8]K. Watari, Y. Seki, and K. Ishizaki, "Temperature Dependence of Thermal Coefficients for HIPed Silicon Nitride," *J. Ceram. Soc. Jpn.* (*Yogyo Kyokaishi*), **97** [2] 174–81 (1989).

[9]T. Hayashi, M. Tamura, T. Hirao, T. Ohashi, and S. Hori, "Silicon Nitride of High Thermal Conductivity," Jpn. Pat. No. 63-86872, Apr. 1988.

[10]K. Hirao, K. Watari, M. E. Brito, M. Toriyama, and S. Kanzaki, "High Thermal Conductivity in Silicon Nitride with Anisotropic Microstructure," *J. Am. Ceram. Soc.*, **79** [9] 2485–88 (1996).

[11]K. Watari, K. Hirao, M. E. Brito, M. Toriyama, and S. Kanzaki, "Hot

Isostatic Pressing to Increase Thermal Conductivity of Si_3N_4 Ceramics," *J. Mater. Res.*, **14** [4] 1538–41 (1999).

[12]N. Hirosaki, Y. Okamoto, M. Ando, F. Munakata, and Y. Akimune, "Effect of Grain Growth on the Thermal Conductivity of Silicon Nitride," *J. Ceram. Soc. Jpn.* (*Yogyo Kyokaishi*), **104** [1] 49–53 (1996).

[13]N. Hirosaki, Y. Okamoto, M. Ando, F. Munakata, and Y. Akimune, "Thermal Conductivity of Gas-Pressure-Sintered Silicon Nitride," *J. Am. Ceram. Soc.*, **79** [11] 2878–82 (1996).

[14]O. Wiener, "Lamellare Doppelbrechung," *Phys. Z.*, **5**, 332–38 (1904).

[15]H. Buhr and G. Müller, "Microstructure and Thermal Conductivity of AlN (Y_2O_3) Ceramics Sintered in Different Atmospheres," *J. Eur. Ceram. Soc.*, **12**, 271–77 (1993).

[16]W.-J. Kim, D. K. Kim, and C. H. Kim, "Morphological Effect of Second Phase on the Thermal Conductivity of AlN Ceramics," *J. Am. Ceram. Soc.*, **79** [4] 1066–72 (1996).

[17]D. R. Clarke and G. Thomas, "Grain-Boundary Phases in Hot-Pressed MgO-Fluxed Silicon Nitride," *J. Am. Ceram. Soc.*, **60** [11–12] 491–95 (1977).

[18]A. Eucken, "Thermal Conductivity of Ceramic Refractory Materials; Calculation from Thermal Conductivities of Constituents," *Forsch. Geb. Ingenieurw.*, **B3** [353] 16 (1932).

[19]W. D. Kingery, H. K. Bowen, and D. R. Uhlmann, *Introduction to Ceramics*, 2nd ed.; pg. 626. Wiley, New York, 1976.

[20]F. F. Lange, "Relation between Strength, Fracture Energy, and Microstructure of Hot-Pressed Si_3N_4," *J. Am. Ceram. Soc.*, **56** [10] 518–22 (1973).

[21]M. Krämer, D. Wittmüss, H. Küppers, M. J. Hoffmann, and G. Petzow, "Relations between Crystal Structure and Growth Morphology of Si_3N_4," *J. Cryst. Growth*, **140**, 157–66 (1994).

[22]H. Buhr, G. Müller, H. Wiggers, F. Aldinger, P. Foley, and A. Roosen, "Phase Composition, Oxygen Content, and Thermal Conductivity of AlN(Y_2O_3) Ceramics," *J. Am. Ceram. Soc.*, **74** [4] 718–23 (1991). □